

CAN RADAR BACKSCATTER RATIO BE USED TO ESTIMATE NDVI AND ACT AS ITS SUBSTITUTE? – A STUDY OVER WINTER WHEAT CROP IN INDIA

Ankur Pandit^{*1}, Suryakant Sawant², Jayantrao Mohite³, Nandan Rajpoot¹, Srinivasu Pappula⁴

¹ Tata Consultancy Services, Research and Innovation, Super Corridor Road, Indore, Madhya Pradesh, India

² Tata Consultancy Services, Tata Research Development and Design Centre (TRDDC), Pune, Maharashtra, India

³ Tata Consultancy Services, Research and Innovation, Pokharan Road, Thane West, Maharashtra, India

⁴ Tata Consultancy Services, Research and Innovation, Hyderabad, Telangana, India

*Corresponding author – ankur.pandit@tcs.com

KEY WORDS: agriculture, wheat, synthetic aperture radar, radar backscatter, NDVI

ABSTRACT:

The Normalised Difference Vegetation Index (NDVI) derived from optical satellite images plays a very important role in determining the state of plants' health. Also, it is an important parameter needed in various statistical/process-based models. However, the use of optical images is sometimes limited because of atmospheric conditions and cloud cover. On the other hand, synthetic aperture radar (SAR) remote sensing has been widely used for crop monitoring due to its high-resolution imaging and all-weather data acquisition capabilities. So, if the SAR backscatter response (σ^0) and NDVI data could be correlated, it is possible to estimate NDVI (during complete or partial stages of crop development) under overcast situations. In this study, three different experiments have been performed to establish the relationship between NDVI- σ^0_{VV} , NDVI- σ^0_{VH} , and NDVI- $\sigma^0_{VV}/\sigma^0_{VH}$. Here, time-series σ^0 (in VV and VH polarizations) and NDVI were extracted from Sentinel-1 and Sentinel-2, respectively. Based on the analysis, it is found that the NDVI is more closely correlated with the ratio $\sigma^0_{VV}/\sigma^0_{VH}$ than it is with σ^0_{VV} and σ^0_{VH} when data points from the start of cropping season up to the start of the maturity stage of the crop, were considered (referred to as experiment 2 and experiment 3). This is opposed to experiment 1, which took into account all data points related to the crop's development i.e. start of cropping season up to the harvesting stage of the crop. The best results were obtained from experiment 3 in which higher-order polynomial regressions were developed between NDVI and $\sigma^0_{VV}/\sigma^0_{VH}$. A significant correlation ranging from $R^2 = 0.81$ to 0.98 were observed for NDVI- $\sigma^0_{VV}/\sigma^0_{VH}$. The study was conducted on selected farms located in the same agro-climatic zone during the Rabi season of 2018-19.

1. INTRODUCTION

Wheat is the primary food ingredient for more than one-third of the world's population (Ortiz et al. 2008). Wheat is also one of the main cereal crops in India. The country is the second largest producer of wheat in the world and the demand for India's wheat in the world shows a rising trend. According to the Ministry of Agriculture & Farmers Welfare, the production of wheat during 2021-22 is estimated at a record 111.32 million tonnes (PIB 2022). As per the Government of India statistics (APEDA 2022), the country has exported around 72 Lakh Metric tonnes of wheat to the world during the year 2021-22. The total value of export was 2,121.72 USD Millions. Wheat cultivation has traditionally been dominated by the northern region of India. Major wheat-growing states in India are Uttar Pradesh, Punjab, Haryana, Madhya Pradesh, Rajasthan, Bihar, and Gujarat. Considering the significance of wheat crop in terms of consumption and commercial matters, continuous monitoring throughout the entire growth stage is crucial. Field measurement techniques were traditionally used to gather information on crop health. Although these techniques often have great accuracy, they might not be suitable for tracking wheat growth in a country having a large area. Hence, satellite Earth observation (EO) data has been extensively utilized globally to monitor different crops and their characteristics over the larger regions. With the help of EO data, a wide range of crop growth dynamic information over the larger region can be obtained promptly. The advantage of EO satellites is their capability to deliver consistent time-series data that can be used to derive important information for precision agricultural applications in a timely manner. Optical as well as Synthetic aperture radar (SAR) EO data have been employed for various agricultural applications. Using such data, different kind of approaches have been developed in the last decades which provides a variety of information on crops.

NDVI, a vegetation index, derived from optical images collected from Landsat-8 and/or Sentinel-2 EO satellites has been widely used in various studies mostly to learn about crop health and growth conditions (e.g. Ghosh et al. 2018; Singh et al. 2020). It is also an important input in various methods employed to quantify parameters such as evapotranspiration (Maselli et al. 2014), Land-cover change detection (Lunetta et al. 2006), and others. However, optical remote sensing images are often affected by clouds and accompanying shadows, which limits further data processing and application (Duan et al. 2020; Xia and Jia 2021). As NDVI is predominantly crucial for agricultural fields, its absence for a long duration can adversely affect the ability to make critical decisions, especially, at crucial times as the crop develops. SAR on the other hand can image both day and night, in almost all weather conditions. Also, SAR remote sensing has certain characteristics and advantages (such as canopy penetrating ability, sensitivity towards the target's geometrical structures and dielectric properties, varying scattering responses for various frequencies and polarizations, etc.) because of which it exhibits significant potential in the field of agricultural remote sensing. However, since it is sensitive to the physical structure of the crop, it does not give a direct indication of the NDVI (Pelta et al. 2022). Also, SAR tends to contain more noise than optical data (Pelta et al. 2022). Therefore, considering the importance of NDVI and its range of utilization, it is important to restore it under cloudy conditions. Therefore, if the SAR backscatter response (σ^0) and NDVI data could be correlated, it is possible to estimate NDVI (during complete or partial stages of crop development) under overcast situations. Several published studies have shown the potential for estimating the NDVI from SAR data using different approaches such as deep learning (e.g. Mazza et al. 2018; Roßberg & Schmitt 2022), Machine Learning (e.g. Mohite et al. 2020; Pelta et al. 2022; Dos Santos et al. 2022), regression algorithms (e.g.

Filgueiras et al. 2019; Holtgrave et al. 2020). These studies have considered the complete stage of crop development (sowing-to-harvest) and evaluated how radar backscatter (in VV and VH polarization) or VV/VH ratio were correlated with NDVI or other vegetation indices. According to our examination of the literature, currently, no studies have addressed the question that till which stage (e.g. sowing-to-maturity) of the wheat crop development, radar backscatter (i.e. σ^{VV} and σ^{VH}) or σ^{VV}/σ^{VH} ratio showing a strong correlation with the NDVI? Also, does that association outweigh the correlation created while taking into account the entire crop development period, from sowing to harvest?

Therefore, in this study, we have attempted to establish the farm-level relationship between (a) NDVI and σ^{VV} (henceforth mentioned as NDVI- σ^{VV}), (b) NDVI and σ^{VH} (henceforth mentioned as NDVI- σ^{VH}), and (c) NDVI and σ^{VV}/σ^{VH} (henceforth mentioned as NDVI- σ^{VV}/σ^{VH}) for the wheat crop. The relationships have been developed under three different experimentations for which data (NDVI and backscatter) were segregated as the two different stages of crop development i.e. sowing-to-harvesting and sowing-to-maturity. These established relationships help us to answer the above-mentioned questions.

2. MATERIALS AND METHODS

1.1 Study Area

The overall study was performed over the selected farms of different shapes and sizes in the Ujjain district of Madhya Pradesh, India. Wheat is an important crop grown in this region. The location of the study farms is shown in Figure 1. Farms boundary was digitized using the high-resolution Google Earth image and given specific names as illustrated in Figure 1. Farms A, B, and C were considered for the development of the relationships for the year 2018-19 whereas Farm D and E were used for validation purposes. All the study farms were having wheat from October 2018 to March 2019. Over the study farms, the sowing was performed in the last week of Oct 2018 whereas the crop was harvested at the end of February or starting of March 2019. Each farm boundary was digitized with a few meters buffer inside the actual boundary to avoid any error occurring due to mixed cropland/non-cropland pixels (Woodcock and Strahler 1987) located at the farm boundary. Basic detail about the crop is mentioned in Table 1.

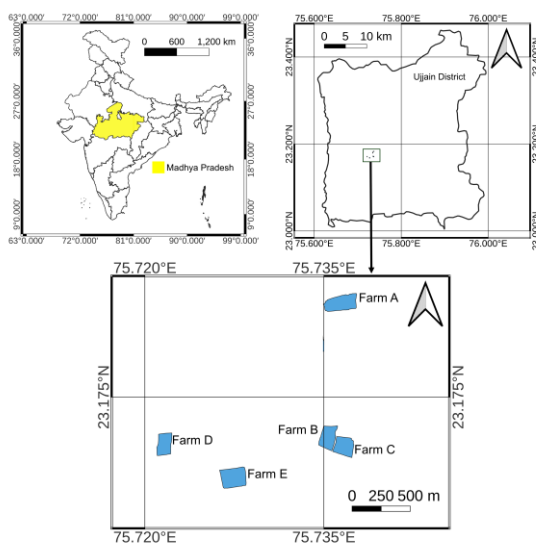


Figure 1. Location of study farms in Ujjain district in Madhya Pradesh, India

Table 1. Basic details about the study crop

Crop Name	Crop Duration (in days)	Max. Crop Height [#] (avg. in cm)	Optimum Mean Temp. (°C)
Wheat (or Triticum aestivum)	90-140 ^a	60-120	21-26

[#]Depending upon the crop variety

1.2 Data used

The current study has used Sentinel-1 and Sentinel-2 satellite data. As part of the Copernicus program of the European Commission (EC), the European Space Agency (ESA) has developed and is currently operating the Sentinel-1 and Sentinel-2 satellite missions. The Sentinel-1 satellite mission provides high-resolution, free, and open-access C-band (at 5.405 GHz) SAR data at the global scale. Each image is acquired in dual-polarization i.e. VV (vertical transmit and vertical receive) and VH (vertical transmit and horizontal receive). The Sentinel-1 mission is capable to map the Indian region in the Interferometric Wide (IW) swath mode once every twelve days. Similarly, Sentinel-2 is a multispectral instrument that provides high-resolution satellite data with thirteen bands once every ten days intervals. Sentinel-1 IW swath mode data of the year 2018-19 of descending flight direction with 136/516 as path/frame and Sentinel-2 L2A data with tile id 43QEF were used in the current study for establishing the relationship between NDVI- σ^{VV} , NDVI- σ^{VH} , and NDVI- σ^{VV}/σ^{VH} . The date of acquisition of Sentinel-1 and Sentinel-2 data are mentioned in Table 2. Here, Sentinel-2 data collected near Sentinel-1 satellite acquisition dates were used to derive NDVI and establish the relationship with σ^{VV} , σ^{VH} , and σ^{VV}/σ^{VH} ratio.

Table 2. Date of acquisition of (a) Sentinel-1 and (b) Sentinel-2 data used in this study

Year	Month	Sentinel-1 Date			Year	Month	Sentinel-2 Date		
2018	Oct	06	18	30	2018	Oct	07	17	
	Nov	11	23			Nov	01	11	21
	Dec	05	17	29		Dec	06	16	31
2019	Jan	10	22		2019	Jan	10	20	30
	Feb	03	27			Feb	24		
	Mar	11	23			Mar	11	21	

(a)

(b)

1.3 Method

In this research, we performed three experiments for establishing relationships between Sentinel-1 (i.e. σ^{VV} , σ^{VH} , and their ratio σ^{VV}/σ^{VH}) and Sentinel-2 (i.e. NDVI) derived indices. In experiment 1 (Exp. 1), all the data points derived during the entire cropping season were considered whereas in experiment 2 (Exp. 2), data points from the start of the cropping season up to the maturity stage of the crop (i.e. browning trend of vegetation greenness or decreasing NDVI), were considered. Both in Exp. 1 and Exp. 2, linear relationships were developed and analyzed. In experiment 3 (Exp. 3), data points that are used in Exp. 2 were utilized to develop 3rd-degree polynomial regression relationships. To evaluate the performance of each estimation model, we adopt the coefficient of determination (R^2) and the root mean squared error (RMSE) which are the most commonly used evaluation metrics. The best model(s) were used to estimate the NDVI of validation farms. At the final stage, the estimated NDVIs were compared with the actual NDVIs and accuracy has been reported. The detailed flowchart of the adopted method is shown in Figure 2.

For the region of interest, Sentinel-1 IW swath Ground Range Detected (GRD) images for the years 2018-19 were used. Radar backscatter in VV (σ^{VV}) and VH (σ^{VH}) polarization were generated using the Hybrid Pluggable Processing Pipeline

(HyP3) platform (Hogenson et al. 2016). It is a programmed SAR data processing online platform that mainly depend on core Amazon services. It provides users with customized on-demand SAR processing services (Agapiou & Lysandrou, 2020). The HyP3 is mainly used to process ESA provided Sentinel-1 data. Based on Alaska Satellite Facility (ASF) data platform, users can search and query the archived Sentinel-1 SAR data based on the region of interest. The HyP3 can automatically access and process these archived data as per the request. In the pre-processing step of SAR data, radiometric calibration, speckle noise removal (i.e. Enhanced Lee filter, window size 7x7) and terrain correction were performed.

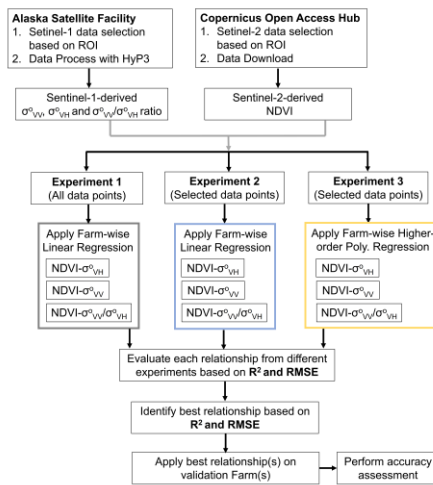


Figure 2. Detailed flow diagram of method adopted for establishing relationship between $NDVI-\sigma^{VV}$, $NDVI-\sigma^{VH}$, and $NDVI-\sigma^{VV}/\sigma^{VH}$

The default outputs (i.e. σ^{VV} and σ^{VH}) of Sentinel-1 RTC products from HyP3 were obtained in power scale, which was further converted into decibels (dB) scale using the Eq. 1. The dB scale brightens the pixels and allows for better differentiation among very dark pixels. The mean of VV and VH in dB units over the study farms was used to determine VV/VH ratio using Eq. 2.

$$\sigma^{o}(dB) = 10 * \log_{10}(\sigma^o) \quad \text{Eq. (1)}$$

$$VV/VH (dB) = \sigma^{VV}(dB) - \sigma^{VH}(dB) \quad \text{Eq. (2)}$$

A total of Fourteen Sentinel-1 images acquired between October 2018 and March 2019 over the study site were used in this study. On the other hand, fourteen time-series Sentinel-2 satellite images for the years 2018-19 were obtained from the Copernicus Open Access Hub (Knowelden and Castriotta 2020) and used to generate the time-series NDVI. The NDVI is typically used to monitor vegetation growth and is considered the proxy measurement of plant photosynthetic activity (Myneni 1997). NDVI operates in the range from (-1) to (+1). Each NDVI output was generated using the combination of Sentinel-2 bands (using Eq. 3).

$$NDVI = \frac{\rho_{NIR-} - \rho_{RED}}{\rho_{NIR+} + \rho_{RED}} \quad \text{Eq. (3)}$$

where ρ_{RED} (0.58–0.68 μm , spectrum range used in the photosynthetic process) and ρ_{NIR} (0.725–1.1 μm , spectrum range with a high reflectance of the internal structures of the leaves) are red and near-infrared channels respectively.

3. RESULTS

This section provides detailed information about the farm-scale relationships developed between $NDVI-\sigma^{VV}$, $NDVI-\sigma^{VH}$, and $NDVI-\sigma^{VV}/\sigma^{VH}$ for all the wheat farms for the Rabi season (i.e. from October to March) of the year 2018. To learn about the development stages of the wheat crop, the NDVI profiles for all the farms were drawn and shown in Figure 3. A similar NDVI trend has been observed for all the farms. Importantly, in this study rather than establishing a relationship at the pixel scale, we have developed it at the farm scale. This is because- 1. Rather than pixel-level, the overall crop health information at a farm scale is crucial in estimating zonal statistics and comparative analysis, 2. A medium-to-coarser resolution satellite image accommodates limited pixels, especially in the small-to-medium size farm. In such a case, a mean value of the indices closely represents the overall farm conditions.

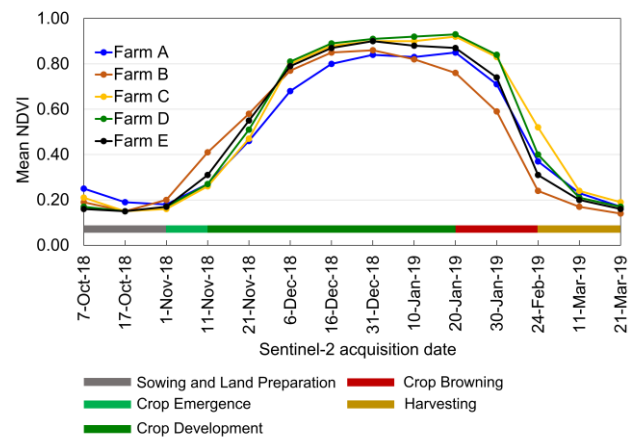


Figure 3. NDVI profile of study farms derived from Sentinel-2

As mentioned in Section 2.3., we have performed three different experiments to establish the relationships between $NDVI-\sigma^{VV}$, $NDVI-\sigma^{VH}$, and $NDVI-\sigma^{VV}/\sigma^{VH}$. Exp. 1 involves all the data points (i.e. NDVI and backscatter) derived during the entire cropping season (sowing-to-harvest) whereas in Exp. 2, data points from the start of the cropping season up to the maturity stage of the crop (browning trend of vegetation greenness or decreasing NDVI), were considered. In both experiments, linear relationships were developed between $NDVI-\sigma^{VV}$, $NDVI-\sigma^{VH}$, and $NDVI-\sigma^{VV}/\sigma^{VH}$. In Exp. 3, the data points considered in Exp. 2 were used and 3rd-degree polynomial relationships were developed. The R^2 values between $NDVI-\sigma^{VV}$, $NDVI-\sigma^{VH}$, and $NDVI-\sigma^{VV}/\sigma^{VH}$ obtained from Exp. 1, 2, and 3 are shown in Table 3.

Table 3. Correlation between $NDVI-\sigma^{VV}$, $NDVI-\sigma^{VH}$, and $NDVI-\sigma^{VV}/\sigma^{VH}$ obtained from Exp. 1, 2, and 3 for Farm A, Farm B, and Farm C

	Experiment 1			Experiment 2			Experiment 3		
Relation Between	A	B	C	A	B	C	A	B	C
$NDVI-\sigma^{VV}$	0.38	0.04	0.11	0.82	0.40	0.49	0.90	0.48	0.63
$NDVI-\sigma^{VH}$	0.23	0.50	0.24	0.02	0.34	0.03	0.04	0.36	0.22
$NDVI-\sigma^{VV}/\sigma^{VH}$	0.69	0.73	0.47	0.91	0.81	0.77	0.94	0.92	0.81

Based on the NDVI analysis (Figure 3), the period of 20-Jan-2019 to 30-Jan-2019 can be considered as the start of the maturity

stage of Farm A, Farm B, Farm C, Farm D, and Farm E. Figure 4 provide high-resolution Google Earth (GE) images of study farms for the cropping season of the years 2018-19. The image dates are close to the Sentinel-1 and Sentinel-2 satellite overpass dates. Greening has been observed for all the farms on 17th Dec 2018. The closest Sentinel-2 observation was available on 16th Dec 2018 on which the NDVI value was 0.80, which also represents greening. Similarly, for the GE image date of 19th Feb 2019, the nearest Sentinel-2 observation was available on 24th Feb 2019 for which the NDVI value was 0.37, which represents the crop maturity stage as seen in the GE image.

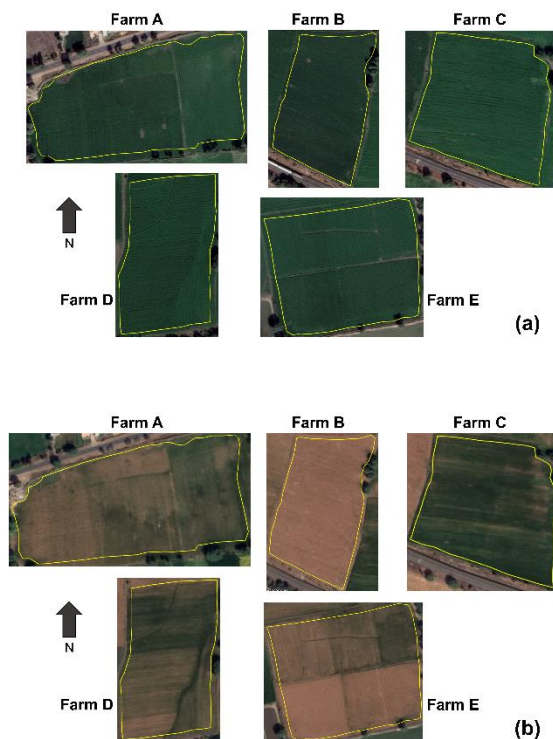


Figure 4. High-resolution images of study farms of (a) 17th Dec 2018 and (b) 19th Feb 2019 obtained for the cropping season of the year 2018-19 (Source: Google, Maxar Technology)

Table 3 provides detail about the correlation obtained from different experiments. Based on the detailed analysis, we found poor R^2 between $NDVI-\sigma_{VV}$ and $NDVI-\sigma_{VH}$ for all the study farms when considering all the data points (i.e. Exp. 1) obtained during the entire cropping season (i.e. from October to March) of the year 2018-19. However, the R^2 between $NDVI-\sigma_{VV}/\sigma_{VH}$ for each farm is comparatively better than the R^2 observations noted for $NDVI-\sigma_{VV}$ and $NDVI-\sigma_{VH}$. In Exp. 2, the R^2 for $NDVI-\sigma_{VV}$ has been improved for each farm. Particularly, for the Farm A and E, the R^2 is above 0.70. On the other hand, it has been observed that the R^2 for $NDVI-\sigma_{VV}/\sigma_{VH}$ has been remarkably improved in Exp. 2 for all the farms as compared to $NDVI-\sigma_{VV}$. Similarly, in Exp. 3, the 3rd-degree polynomial relationship shows much better R^2 in the case of $NDVI-\sigma_{VV}$ and $NDVI-\sigma_{VV}/\sigma_{VH}$ as compared to Exp. 1 and 2. However, it is important to highlight that the R^2 for $NDVI-\sigma_{VH}$ has been consistently poor in all three experiments. Based on the detailed analysis of Exp.1, 2, and 3, we found that the NDVI is having a poor correlation with both σ_{VV} and σ_{VV}/σ_{VH} when the crop reached the maturity stage. This particular observation has been valid for all the training farms. Certain factors may affect the $NDVI-\sigma_{VV}$ and $NDVI-\sigma_{VV}/\sigma_{VH}$ relationships during the crop development stage- Firstly, a certain time lag (not more than three days) was observed

in Sentinel-1 and Sentinel-2 satellite data acquisition for the year 2018-19. Therefore, the ground conditions may not be identical in the Sentinel-1 and Sentinel-2 images. However, in the current study, this may impact the correlation to a very limited extent as the gap is not very wide. Moreover, it is not always possible to have Sentinel-1 and Sentinel-2 satellite data acquisition on the same date for a particular region. Secondly, after maturity, farms are usually harvested part-by-part or completely depending upon the size of the farm using different harvesting techniques. This could result in non-uniformity on the farm, leaving some areas exposed to soil, and/or rest covered in a crop. Because of such reasons, the σ_{VV} and σ_{VV}/σ_{VH} could not develop a good correlation with NDVI after the crop maturity stage.

For the validation purpose, the higher-order polynomial relationships (refer Figure 5) developed between $NDVI-\sigma_{VV}/\sigma_{VH}$ in Exp. 3 were applied over Farm D and Farm E lies in the same region. The time-series NDVI were re-generated for Farm D and Farm E using the relationships and compared with the actual NDVI obtained from Sentinel-2 data. Figure 6 represent the actual and estimated NDVI profiles obtained for Farm D and Farm E. A similar trend as of actual NDVI was observed in the case of estimated NDVI. However, in the case of Farm E, a sudden fall in the estimated NDVI was observed due to the abrupt dropping of the σ_{VV} component (from -14.25 to -15.21) of σ_{VV}/σ_{VH} , which needs further investigation. In the case of Farm D, the R^2 were ranging from 0.79 to 0.92 whereas RMSE were ranging from 0.14 to 0.17. Similarly, for Farm E, the R^2 were ranging from 0.70 to 0.84 whereas RMSE were ranging from 0.13 to 0.18. The NDVI estimated using the Farm B equation showed a strong correlation with the actual NDVI as compared to other farm equations.

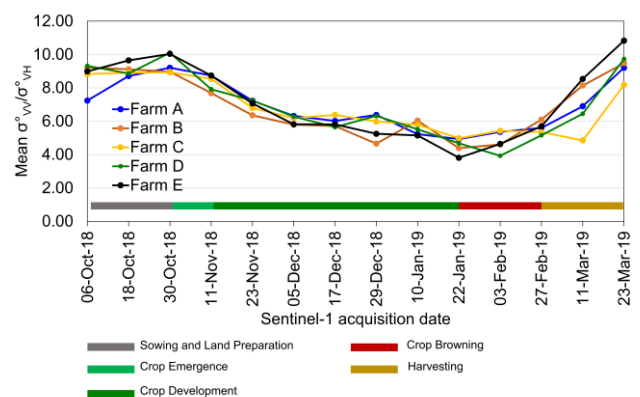


Figure 7. Time-series profile of σ_{VV}/σ_{VH} of all the study farms for the year 2018-19 for entire cropping duration (sowing-to-harvest).

In addition to the aforesaid analysis, a time-series σ_{VV}/σ_{VH} profile (see Figure 7) was created to determine whether it exhibited any similarities to the NDVI profile during the cropping period (i.e. sowing-to-harvest). We found that σ_{VV}/σ_{VH} can explain various crop development stages like NDVI by following the inverse profile of NDVI throughout the season. From the comparative analysis point of view, the following observations were noted from both the time-series profiles-

1. The initial observation of the NDVI profile (refer Figure 3) likely represents the land preparation and sowing activities from October 7 to November 1, 2018. The study farms' NDVI over that period (refer Figure 3) was consistently low. The tillage activities that were performed across the farms before the sowing of the fresh crop are represented by a lower

NDVI. All of the farms observed a noticeable change in $\sigma_{VV}^0/\sigma_{VH}^0$ (from low to high) throughout the same period (i.e., from October 6th to October 18th, 2018 of Sentinel-1) (refer Figure 7). Such variations in the radar backscatter were observed because SAR signals are highly sensitive toward the soil roughness, which in agricultural fields is affected by the characteristics of tillage operations. (Ulaby and Bare, 1979). Moreover, in the early stage of growth, soil played a leading role in radar backscatter (McNairn et al. 2009).

- Next, the shift in the NDVI values (from low to high) from November 1st to 11th 2018 represents vegetation emergence that took place anytime between those dates of the year 2018-19 (refer Figure 3). For all the farms, as discussed, the $\sigma_{VV}^0/\sigma_{VH}^0$ profile (refer Figure 7) follows the reverse of NDVI patterns that appeared between 30th October and 11th November 2018.
- The NDVI trend from 11th November 2018 to 30th January 2019 (refer Figure 3) represents crop growth duration. An analogous but inverse trend was also observed in the $\sigma_{VV}^0/\sigma_{VH}^0$ profile (refer Figure 7) for the same duration (i.e. 11th November 2018 to 03rd February 2019). Between 16th December 2018 and 20th January 2019, study farms reached to peak vegetative stage as observed in the NDVI profile (≥ 0.80) for the year 2018-19. For the same period, the lowest $\sigma_{VV}^0/\sigma_{VH}^0$ values have been observed, which represents the peak vegetative stage of wheat. Importantly, during the growth stage, crop more uniformly covered the ground surface hence, the surface scattering decreased gradually, and the backscatter value decreased with the increase of the leaf density (Zhou et al. 2017).
- Between 20th and 30th January 2019, NDVI analysis (see Figure 3) shows that the crop reached the browning stage at all the farms (see Figure 4b also). This stage is related to physiological maturity, leading to the senescence of leaves. Change in $\sigma_{VV}^0/\sigma_{VH}^0$ (low to high) started between 20th January and 03rd February 2019, representing the same. It is important to highlight here that in Exp. 3, we have not considered the data points mostly after 30th January 2019. This is because, poor correlation was observed when considering those data points.
- Between 24th Feb and 21st Mar 2019, the crop was mostly harvested from all the farms as depicted from the NDVI profile for the year 2018-19 (refer Figure 3). Changes in $\sigma_{VV}^0/\sigma_{VH}^0$ (low to high) (refer Figure 7) from 27th Feb to 23rd Mar 2019 represents similar observations as seen in NDVI. Following 03rd Feb 2019, the next Sentinel-1 data was available on 27th Feb 2019 (i.e. after a twenty-four days gap). One observation was missing between the 03rd and 27th Feb 2019. The gap probably represents the further browning of vegetation after 03rd Feb 2019.

4. CONCLUSION

Based on the analysis, NDVI- $\sigma_{VV}^0/\sigma_{VH}^0$ was found to have a better correlation than NDVI- σ_{VV}^0 and NDVI- σ_{VH}^0 in both linear regression and higher-order polynomial regression. In addition, we discovered that third-order polynomial regression, as opposed to linear regression, better describes a nonlinear relationship between NDVI and $\sigma_{VV}^0/\sigma_{VH}^0$. This strong correlation exists while considering the data points (i.e. NDVI and σ_{VV}^0) from the start of the cropping season up to the maturity stage of the wheat crop, beyond that strong correlation does not exist. Hence, under cloudy conditions, $\sigma_{VV}^0/\sigma_{VH}^0$ can be used to estimate the NDVI during the crucial crop growth stages (i.e. sowing to maturity). Also, current study demonstrated that the prominent variations in time-series $\sigma_{VV}^0/\sigma_{VH}^0$ well describe the crop growth stages and the overall trend in $\sigma_{VV}^0/\sigma_{VH}^0$ is in agreement with the NDVI

profile. Considering the cost and frequency of data acquisition over the region, utilization of C-band SAR data can overcome the user's dependency on optical remote sensing, which is not capable to capture the earth's imagery during the presence of cloud cover over the study region. Since there were few data points available throughout the cropping season, it would be easier to comprehend the relationship between NDVI- $\sigma_{VV}^0/\sigma_{VH}^0$ if Sentinel-1/2 satellite data were more frequently available for the study region.

REFERENCES

- Agapiou, A.; Lysandrou, V., 2020: Detecting Displacements Within Archaeological Sites in Cyprus After a 5.6 Magnitude Scale Earthquake Event Through the Hybrid Pluggable Processing Pipeline (HyP3) Cloud-Based System and Sentinel-1 Interferometric Synthetic Aperture Radar (InSAR) Analysis. *IEEE J. Sel. Top. Appl. Earth Obs. Remote Sens.* 2020, 13, 6115–6123
- APEDA (2022) https://apeda.gov.in/apedawebsite/SubHead_Products/Wheat.htm
- Dos Santos, E. P., da Silva, D. D., do Amaral, C. H., Fernandes-Filho, E. I., Dias, R. L. S., 2022: A Machine Learning approach to reconstruct cloudy affected vegetation indices imagery via data fusion from Sentinel-1 and Landsat 8. *Computers and Electronics in Agriculture*, 194, 106753.
- Duan, C., Pan, J., Li, R., 2020: Thick cloud removal of remote sensing images using temporal smoothness and sparsity regularized tensor optimization. *Remote Sensing*, 12(20), 3446.
- Filgueiras, R., Mantovani, E. C., Althoff, D., Fernandes Filho, E. I., Cunha, F. F. D. 2019: Crop NDVI monitoring based on sentinel 1. *Remote Sensing*, 11(12), 1441.
- Ghosh, P., Mandal, D., Bhattacharya, A., Nanda, M. K., & Bera, S. (2018). Assessing crop monitoring potential of Sentinel-2 in a spatio-temporal scale. *The International Archives of Photogrammetry, Remote Sensing and Spatial Information Sciences*, 42, 227-231.
- Holtgrave, A. K., Röder, N., Ackermann, A., Erasmi, S., Kleinschmit, B., 2020: Comparing Sentinel-1 and-2 data and indices for agricultural land use monitoring. *Remote Sensing*, 12(18), 2919.
- Hogenson, K., Arko, S. A., Buechler, B., Hogenson, R., Herrmann, J., & Geiger, A., 2016: Hybrid Pluggable Processing Pipeline (HyP3): A cloud-based infrastructure for generic processing of SAR data. In *Agu fall meeting abstracts*.
- Lunetta, R. S., Knight, J. F., Ediriwickrema, J., Lyon, J. G., & Worthy, L. D., 2006: Land-cover change detection using multi-temporal MODIS NDVI data. *Remote sensing of Environment*, 105(2), 142-154.
- Maselli, F., Papale, D., Chiesi, M., Matteucci, G., Angeli, L., Raschi, A., Seufert, G., 2014: Operational monitoring of daily evapotranspiration by the combination of MODIS NDVI and ground meteorological data: Application and evaluation in Central Italy. *Remote Sensing of Environment*, 152, 279-290.
- Mazza, A., Gargiulo, M., Scarpa, G., Gaetano, R., 2018: Estimating the NDVI from SAR by convolutional neural networks. In *IGARSS 2018-2018 IEEE International Geoscience and Remote Sensing Symposium*, 1954-1957.
- McNairn, H., Champagne, C., Shang, J., Holmstrom, D., Reichert, G., 2009: Integration of optical and Synthetic Aperture Radar (SAR) imagery for delivering operational

annual crop inventories. *ISPRS J. Photogramm. Remote Sens.*, 64, 434–449.

Mohite, J. D., Sawant, S. A., Pandit, A., Pappula, S., 2020: Investigating the Performance of Random Forest and Support Vector Regression for Estimation of Cloud-Free NDVI using SENTINEL-1 SAR Data. *The International Archives of Photogrammetry, Remote Sensing and Spatial Information Sciences*, 43, 1379-1383.

Ortiz, R., Sayre, K. D., Govaerts, B., Gupta, R., Subbarao, G. V., Ban, T., ... Reynolds, M., 2008: Climate change: can wheat beat the heat?. *Agriculture, Ecosystems & Environment*, 126(1-2), 46-58.

Pelta, R., Beeri, O., Tarshish, R., Shilo, T., 2022: Sentinel-1 to NDVI for agricultural fields using hyperlocal dynamic machine learning approach. *Remote Sensing*, 14(11), 2600.

PIB (2022). <https://pib.gov.in/PressReleasePage.aspx?PRID=1798835>

Roßberg, T., Schmitt, M., 2022: Estimating NDVI from Sentinel-1 SAR Data using Deep Learning. *In IGARSS 2022-2022 IEEE International Geoscience and Remote Sensing Symposium*. 1412-1415.

Singh, B. M., Komal, C., Victorovich, K. A., 2020: Crop growth monitoring through Sentinel and Landsat data based NDVI time-series. *Comput. Opt.* 2020, 44, 409–419.

Ulaby, F. T., Moore, R. K., Fung, A. K., 1986: *Microwave Remote Sensing*. Vol. 3, Active and Passive. Boston, MA: Artech House,

Ulaby F.T., Bare J.E. 1979: Look direction modulation function of the radar backscattering coefficient of agricultural fields. *Photogrammetric Engineering and Remote Sensing*, 45, 1495–1506.

Woodcock, C. E., Strahler, A. H., 1987: The factor of scale in remote sensing. *Remote sensing of Environment*, 21(3), 311-332.

Xia, M., Jia, K., 2021: Reconstructing Missing Information of Remote Sensing Data Contaminated by Large and Thick Clouds Based on an Improved Multitemporal Dictionary Learning Method. *IEEE Transactions on Geoscience and Remote Sensing*, 60, 1-14.

Zhou, T., Pan, J., Zhang, P., Wei, S., Han, T., 2017: Mapping winter wheat with multi-temporal SAR and optical images in an urban agricultural region. *Sensors*, 17(6), 1210.

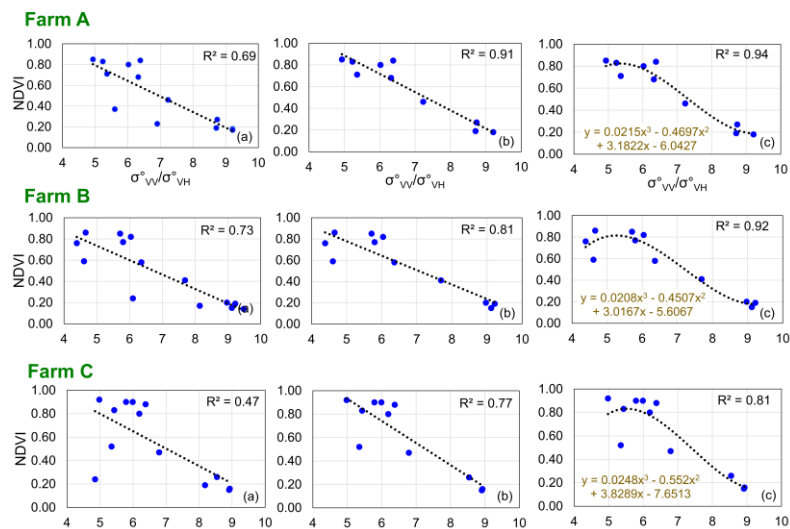


Figure 5. Relationships between NDVI- $\sigma^0_{VV}/\sigma^0_{VH}$ for study farms for the year 2018-19. All the left-hand side figures represent the correlation obtained from Exp. 1 whereas the figures at the middle represents correlation from Exp. 2. The figures on the right-hand side show correlation obtained from Exp. 3.

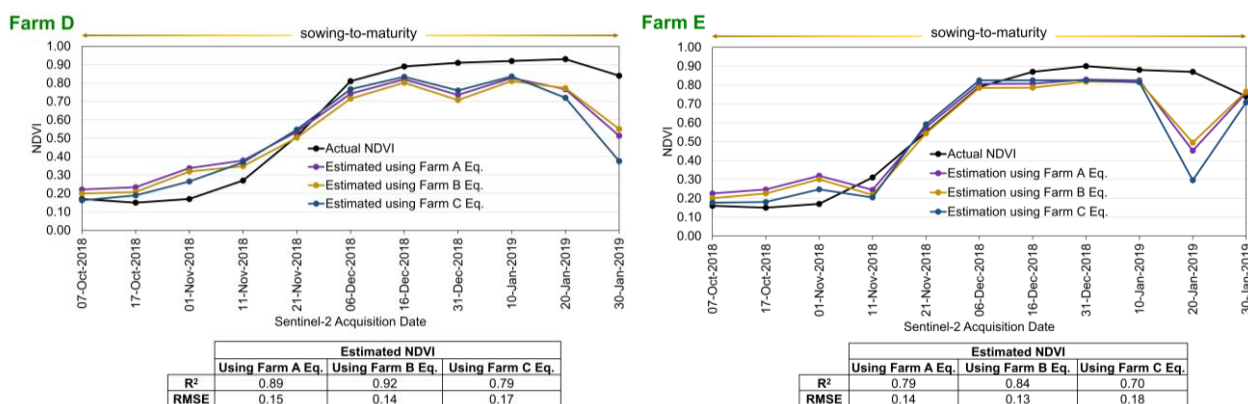


Figure 6. Actual vs Estimated NDVI for the Farm D and Farm E. NDVI was estimated using the equations derived for Farm A, B and C. Model evaluation metrics i.e. R^2 and RMSE for the Farm D and Farm E are also shown here.